Acta Crystallographica Section F
Structural Biology Communications
ISSN 2053-230X

Structure determination of BA0150, a putative polysaccharide deacetylase from *Bacillus anthracis*

Robert J. Strunk,[a] Katrina M. Piemonte,[a] Natasha M. Petersen,[a] Dimitris Koutsioulis,[b] Vassilis Bouriotis,[b,c] Kay Perry[d]* and Kathryn E. Cole[a]*‡

[a]Department of Chemistry, Ithaca College, 953 Danby Road, Ithaca, NY 14850, USA, [b]Department of Biology, Enzyme Biotechnology Group, University of Crete, PO Box 2209, Vassilika Vouton, 71409 Heraklion, Crete, Greece, [c]Institute of Molecular Biology and Biotechnology, 70019 Heraklion, Crete, Greece, and [d]Northeastern Collaborative Access Team (NE-CAT) and Department of Chemistry and Chemical Biology, Cornell University, Building 436E, Argonne National Laboratory, 9700 South Cass Avenue, Argonne, IL 60439, USA

‡ Current address: Department of Molecular Biology and Chemistry, Christopher Newport University, 1 Avenue of the Arts, Newport News, VA 23606, USA.

Correspondence e-mail: kperry@anl.gov, kathryn.cole@cnu.edu

Received 26 September 2013
Accepted 19 December 2013

PDB reference: BA0150, 4m1b

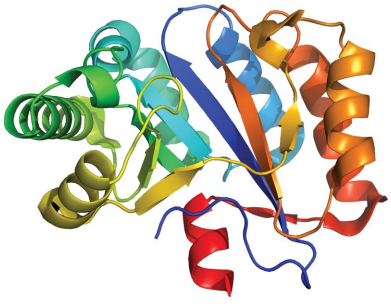

Polysaccharide deacetylases are bacterial enzymes that catalyze the deacetylation of acetylated sugars on the membranes of Gram-positive bacteria, allowing them to be unrecognized by host immune systems. Inhibition of these enzymes would disrupt such pathogenic defensive mechanisms and therefore offers a promising route for the development of novel antibiotic therapeutics. Here, the first X-ray crystal structure of BA0150, a putative polysaccharide deacetylase from *Bacillus anthracis*, is reported to 2.0 Å resolution. The overall structure maintains the conserved $(\alpha/\beta)_8$ fold that is characteristic of this family of enzymes. The lack of a catalytic metal ion and a distinctive metal-binding site, however, suggest that this enzyme is not a functional polysaccharide deacetylase.

1. Introduction

Polysaccharide deacetylases (PDs) are family 4 carbohydrate esterases (CE-4) found in bacteria, and include acetyl xylan esterases, chitin deacetylases, chitooligosaccharide deacetylases and peptidoglycan deacetylases (Caufrier *et al.*, 2003; Davies *et al.*, 2005). These enzymes catalyze the *N*- or *O*-deacetylation of acetylated sugars on the membranes of Gram-positive bacteria. In altering their membrane recognition, the bacteria become invisible to mammalian hydrolases, such as lysozyme, and defend themselves against host immune systems (Boneca, 2005). These enzymes are so critical for bacterial virulence that the genomes of *Bacillus anthracis* and its close homolog *B. cereus* both encode at least ten PDs (Psylinakis *et al.*, 2005). Deletion of the peptidoglycan *N*-acetylglucosamine deacetylase A gene (*pgdA*) resulted in the bacteria being more susceptible to lysozyme (Vollmer & Tomasz, 2000; Boneca *et al.*, 2007), and deletion of *pgdA* in *Streptococcus pneumoniae* specifically caused the pathogen to become less infective in a mouse model (Vollmer & Tomasz, 2002). Inhibition of PDs will similarly thwart such bacterial defensive mechanisms, and offers a promising route for the development of novel antibiotic therapeutics and/or prophylatic drugs. This information is especially crucial as we consider the threat of bioterrorism and potentially weaponizable bacteria in the present day.

In order to be effective against a wide range of pathogenic bacteria, an inhibitor should target conserved enzyme features, such as folds, surfaces and catalytic metal ions. Although the CE-4 enzymes share relatively low sequence identities, the available crystal structures reveal a conserved $(\alpha/\beta)_8$-barrel fold, termed the NodB homology domain for its likeness to NodB proteins (Kafetzopoulos *et al.*, 1993; Blair & van Aalten, 2004; Blair *et al.*, 2005; Taylor *et al.*, 2006; Oberbarnscheidt *et al.*, 2007; Deng *et al.*, 2009; Fadouloglou *et al.*, 2013; PDB entry 1ny1, Northeast Structural Genomics Consortium, unpublished work; PDB entry 3rzx, Midwest Center for Structural Genomics, unpublished work). In addition, a divalent metal ion (typically zinc) that is required for enzyme activity is found in the active site coordinated by a largely conserved Asp–His–His motif (Blair *et al.*, 2005). The metal coordination sphere is completed by exogenous anions from the crystallization conditions (acetate, cacodylate, phosphate *etc.*) in the known structures. The proposed general acid/base mechanism of deacetylation is thought to be similar to that

Table 1
Data-collection and structure-refinement statistics for BA0150.

Values in parentheses are for the highest resolution shell.

Data collection	
Resolution range (Å)	48.11–2.00 (2.11–2.00)
Space group	$P2_12_12_1$
Unit-cell parameters (Å)	a = 47.14, b = 75.79, c = 124.54
R_{merge}†	0.081 (0.548)
R_{meas}‡	0.096 (0.683)
Completeness (%)	99.2 (95.9)
Multiplicity	5.9 (3.7)
$\langle I/\sigma(I)\rangle$	16.4 (2.4)
No. of reflections	181499
No. of unique reflections	30744
Mosaicity (°)	0.19
Refinement	
R_{work}/R_{free}§	0.17/0.21
No. of atoms	
Protein	3156
Polyethylene glycol	10
Water	295
B factors (Å^2)	
Overall	28.8
Protein	28.0
Polyethylene glycol	44.5
Water	36.5
R.m.s.d.s	
Bond lengths (Å)	0.007
Bond angles (°)	1.040
Ramachandran statistics (%)	
Preferred	98
Allowed	2
Outliers	0

† $R_{merge} = \sum_{hkl}\sum_i |I_i(hkl) - \langle I(hkl)\rangle| / \sum_{hkl}\sum_i I_i(hkl)$, where $I_i(hkl)$ is the ith observation of reflection hkl and $\langle I(hkl)\rangle$ is the weighted average intensity for all observations i of reflection hkl. ‡ $R_{meas} = \sum_{hkl}\{1/[N(hkl)-1]\}^{1/2}\sum_i |I_i(hkl) - \langle I(hkl)\rangle| / \sum_{hkl}\sum_i I_i(hkl)$, where R_{meas} is a merging R factor independent of data redundancy. § $R_{work} = \sum_{hkl} \big||F_{obs}| - |F_{calc}|\big| / \sum_{hkl} |F_{obs}|$, where F_{obs} and F_{calc} are the observed and calculated structure factors, respectively, and the statistic is calculated for all reflections except for the test set. R_{free} is calculated accordingly for reflections excluded from refinement (the test set).

of other zinc-dependent deacetylases (Blair *et al.*, 2005; Hernick & Fierke, 2005).

Here, we report the first X-ray crystal structure of BA0150, a putative PD from *B. anthracis*, to 2.0 Å resolution. The overall structure of BA0150 is similar to other known structures and reveals the conserved $(\alpha/\beta)_8$ fold that is characteristic of this family of enzymes. Notably, however, BA0150 lacks the conserved Asp–His–His metal-binding motif and a catalytic metal ion, suggesting that it is not a functional PD.

2. Materials and methods

2.1. Protein expression and purification

The BA0150 plasmid was a gift from Professor Vassilis Bouriotis (University of Crete); the construct encodes BA0150 (∼28 500 kDa) with a C-terminal His tag. BA0150 was recombinantly expressed in *Escherichia coli* BL21(DE3)pLysS cells. The cells were grown in LB medium supplemented with kanamycin (50 µg l^{-1}) at 37°C for ∼3 h, at which point the cells were induced by the addition of isopropyl β-D-1-thiogalactopyranoside (0.3 m*M* final concentration) and grown for ∼6 h at 37°C. The cells were pelleted by centrifugation, resuspended in 25 ml buffer *A* (50 m*M* Tris pH 7.6, 200 m*M* NaCl, 10% glycerol) and lysed by sonication on ice. The cell debris was pelleted by centrifugation and the cell-free extract was purified using affinity chromatography (Talon Cobalt resin; buffer *A*, as above; buffer *B*, 50 m*M* Tris base pH 7.6, 200 m*M* NaCl, 10% glycerol, 500 m*M* imidazole) and size-exclusion chromatography (HiLoad 26/60 Superdex, GE Healthcare) in 25 m*M* Tris base pH 8.0, 300 m*M* NaCl, 10% glycerol. The final yield was >200 mg l^{-1} and the final purity of BA0150 was >95% as determined by SDS–PAGE. The concentration of BA0150 was determined from its absorbance using a calculated extinction coefficient (ε_{280} = 37 410 M^{-1} cm^{-1}; Gill & von Hippel, 1989).

2.2. Crystallization and data collection

Clusters of rectangular crystals were obtained in 1–2 d using the hanging-drop vapor-diffusion method with the following conditions: 2 µl protein solution (24–28 mg ml^{-1} BA0150 in 25 m*M* Tris base pH 8.0, 300 m*M* NaCl, 10% glycerol) were mixed with 2 µl precipitant solution (0.1 *M* Tris base pH 8.0, 0.2 *M* NaCl, 30–34% PEG 3350) and equilibrated against a 500 µl reservoir of precipitant solution. Single crystals were harvested and flash-cooled using the precipitant buffer supplemented with 20% glycerol. Crystals diffracted X-rays to 2.0 Å resolution on the Advanced Photon Source beamline NE-CAT 24-ID-C (Argonne National Laboratory) with a Pilatus 6MF detector. Diffraction data were indexed and scaled using *XDS* as implemented in the *Rapid Automated Processing of X-ray Data* package (https://github.com/RAPD/RAPD). The crystals belonged to space group $P2_12_12_1$, with unit-cell parameters a = 47.14, b = 75.79, c = 124.54 Å.

2.3. Energy-dispersive X-ray spectroscopy

Elemental analysis of cryogenically protected BA0150 crystals was performed on NE-CAT 24-ID-C using an Amptek X-123SDD silicon drift detector. X-ray excitation of the crystals occurred at 12 662 eV. Fluorescence emission amplitudes were detected from 6000 to 13 000 eV. Only Compton scattering from the excitation was observed.

2.4. Structure determination and refinement

The structure was determined using an *HHpred* alignment and *Rosetta* as implemented in *PHENIX* (Terwilliger *et al.*, 2012) on a TeamHPC 128-core computing cluster. The Matthews coefficient predicted a single molecule in the asymmetric unit, but successful molecular replacement using a carbohydrate esterase from *B. anthracis* (30% sequence identity; PDB entry 2j13; Oberbarnscheidt *et al.*, 2007) and *phenix.mr_rosetta* required the explicit statement of two molecules in the asymmetric unit. This resulted in a solvent content of 37%. *Phenix.mr_rosetta* produced a model with an R_{work} of 0.24 and an R_{free} of 0.29. The model was refined using iterative cycles of refinement in *PHENIX* (Adams *et al.*, 2002) and manual model rebuilding in *Coot* (Emsley & Cowtan, 2004). *Coot* was used to define secondary-structural elements in *PyMOL* (v.0.99rc6; Schrödinger). Disordered segments in the final model include Met1–Pro46 and Ser247–Gln254 in both monomers *A* and *B*. Data-collection and refinement statistics are given in Table 1. The atomic coordinates and structure factors of BA0150 have been deposited in the Protein Data Bank (http://www.rcsb.org) with accession code 4m1b.

3. Results and discussion

Here, we report the first X-ray crystal structure of BA0150, a putative PD from *B. anthracis*, to 2.0 Å resolution. The structure was determined using an *HHpred* alignment and *phenix.mr_rosetta* (Terwilliger *et al.*, 2012) with two molecules in the asymmetric unit, resulting in a solvent content of 37%. The two independent monomers of BA0150 in the $P2_12_12_1$ unit cell are structurally quite similar, with r.m.s. deviations of 0.86 Å for 200 C$^\alpha$ atoms and 1.38 Å for all atoms (Maiti

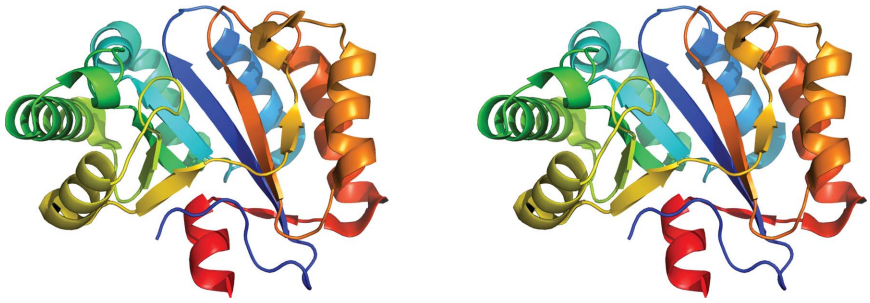

Figure 1
Stereoview of monomer *A* of BA0150. The monomer is colored in 'chainbows' to highlight the secondary structure of the NodB domain.

```
PDB_2J13      TFDNGYENGYTGKILDVLKEKKVP---ATFFVTGHYIKTQKD-LLLRMKDEGHIIGNHSW
PDB_2Y8U      TFDDGPS-EYTPQLLDLLSRYSAR---ATFFVLGDAAAQNPG-LLQRMRDEGHQVGAHTY
PDB_2CC0      TFDDGPS-GSTQSLLNALRQNGLR---ATMFNQGQYAAQNPS-LVRAQVDAGMWVANHSY
PDB_2C1G      TFDDGPNPATTPQVLETLAKYDIK---ATFFVLGKNVSGNED-LVKRIKSEGHVVGNHSW
BA0150        TFDISWGDKKAIPILDTLKERDIKN--ATFFLSAAWAERHPD-VVERIIKDGHEIGSMGY
PDB_2W3Z      TFDDGVDPNMTPKILDVLAQQHVH---ATFFLVGCNITDKVKPILQRQITEGHALGIHSF
PDB_3RXZ*     SHQAYGPLVGVPRLLGILDEFNVP---GTFFVPGYTAHRHPE-PIRSIARAGHEIAHHGY
PDB_4HD5*     EATGMKEDGKTIPLTKSIITFEQKVPVLMYHAIDDYHGQGIKDLFVSPANFEAQMKHLKD

PDB_2J13      SHPDFTAVN-----DEKLREELTSVTEEIKKVTGQKEVK-YVRPPRGVFSERTLALTKEM
PDB_2Y8U      DHVSLPSLG-----YDGIASQMTRLEEVIRPALG-VAPA-YMRPPYLETNELVLQVMRDL
PDB_2CC0      THPHMTQLG-----QAQMDSEISRTQQAIAGAGG-GTPK-LFRPPYGETNATLRSVEAKY
PDB_2C1G      SHPILSQLS-----LDEAKKQITDTEDVLTKVLG-SSSK-LMRPPYGAITDDIR---NSL
BA0150        NYTSYTSLE-----TNEIRRDLLRAQDVFTKLG-VKQIK-LLRPPSGDFNKATLKIAESL
PDB_2W3Z      SHVYSLLYPNRVGNTQQIVSEVTRTQNALKDQLGQNFKTGVWRYPGG---HLSWTGLEAA
PDB_3RXZ*     LHESLVGAD-----EDTERKILTRGIEALEEVAGVHPVG--YRAPMWEMNWHTPKLLAEF
PDB_4HD5*     NGYTLLTFERWGDINKVNKPIFVTFDDGMKNNMNAFRVLQKLKDDTFKPAATEYMIVDNV

*3RXZ Asp residue upstream and 4HD5 His residues downstream of shown sequence
```

Figure 2
Partial sequence alignments of structurally characterized PDs from Gram-positive bacteria that contain metal ions in the active sites. Largely conserved residues are shown in bold and underlined. The largely conserved Asp–His–His metal-binding residues are shown in bold.

et al., 2004). A polyethylene glycol molecule was modeled into density in monomer *B* (not shown). The structure of monomer *A* is shown in Fig. 1. The conserved $(\alpha/\beta)_8$-barrel homology domain is clearly visible, and the overall structure aligns well with other known PD structures from Gram-positive bacteria.

Interestingly, however, the crystal structure does not contain a catalytic metal ion. While most PDs have a metal ion (typically zinc) that is required for enzyme activity, three independent data collections have shown that BA0150 reproducibly crystallizes as an apoenzyme under the reported conditions. Energy-dispersive X-ray spectroscopy confirmed the complete absence of any metals in the protein crystals. Sequence alignments show that BA0150 does not contain the conserved Asp–His–His metal-binding triad that is found in many CE-4 enzymes (Blair *et al.*, 2005). Fig. 2 is a partial sequence alignment of the structurally characterized PDs from Gram-positive bacteria that contain a metal ion in the active site. Rather than the Asp–His–His triad, BA0150 contains Ile, Met and Tyr residues in the metal-binding sites, respectively, none of which have a strong affinity for metal binding (Fig. 3). Furthermore, the Ile residue points away from the putative active site and makes long-range hydrophobic interactions with Ala72, Trp95 and Ala211. Crystallization trials using a zinc salt (50–200 m*M* $ZnCl_2$) in place of NaCl largely resulted in protein precipitation, and zinc-soaking experiments with pre-formed crystals (0.5–5 m*M* $ZnCl_2$, ∼2 h) failed to produce any zinc anomalous signal or zinc difference density in the active site. The inability to bind metal suggests that BA0150 is not a metalloenzyme and, in fact, is not a functional PD. While the catalytic metal ion is missing, the putative active site has nearby Asp (Asp64) and His (His210) residues, which are largely conserved among the PDs, and suggests that the enzyme may have some hydrolytic activity. Studies to measure activity and determine specific functionality are in progress.

4. Conclusions

In summary, we report the first X-ray crystal structure of BA0150. The overall structure reveals that the protein maintains the conserved $(\alpha/\beta)_8$ barrel (NodB domain) that is characteristic of the CE-4 family

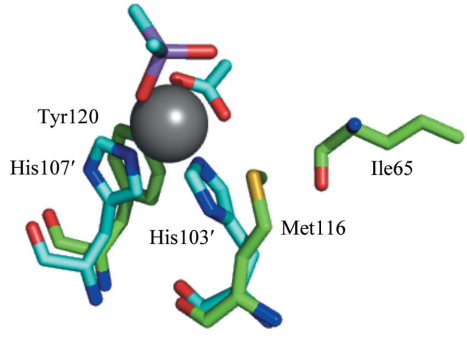

Figure 3
Active-site alignment of BA0150 with a carbohydrate esterase from *B. anthracis* (PDB entry 2j13). The active-site residues in BA0150 are Ile65, Met116 and Tyr120 (C, green; N, blue; O, red; S, yellow). The active-site residues in 2j13 are His103 and His107, with metal coordination completed by acetate and cacodylate anions (C, cyan; N, blue; O, red; As, purple). The catalytic zinc ion of 2j13 is shown as a gray sphere.

of enzymes. The enzyme reproducibly crystallized without a catalytic metal, however; the lack of the conserved Asp-His-His triad indicates that this enzyme is not a metalloenzyme and is not a functional PD. The largely conserved Asp and His residues near the putative active site, however, suggest that BA0150 may have some hydrolytic activity. Studies to determine specific functionality are ongoing.

The work of DK and VB was co-financed by EU (ERDF) and Greek funds through the 'THALIS' program. This work is based upon research conducted at the Advanced Photon Source on the Northeastern Collaborative Access Team beamlines, which are supported by a grant from the National Institute of General Medical Sciences (P41 GM103403) of the National Institutes of Health. Use of the Advanced Photon Source, an Office of Science User Facility operated for the US Department of Energy (DOE) Office of Science by Argonne National Laboratory, was supported by the US DOE under Contract No. DE-AC02-06CH11357. KEC and RJS would like to thank Ithaca College for funding.

References

Adams, P. D., Grosse-Kunstleve, R. W., Hung, L.-W., Ioerger, T. R., McCoy, A. J., Moriarty, N. W., Read, R. J., Sacchettini, J. C., Sauter, N. K. & Terwilliger, T. C. (2002). *Acta Cryst.* D**58**, 1948–1954.
Blair, D. E., Schüttelkopf, A. W., MacRae, J. I. & van Aalten, D. M. F. (2005). *Proc. Natl Acad. Sci. USA*, **102**, 15429–15434.
Blair, D. E. & van Aalten, D. M. F. (2004). *FEBS Lett.* **570**, 13–19.
Boneca, I. G. (2005). *Curr. Opin. Microbiol.* **8**, 46–53.
Boneca, I. G. *et al.* (2007). *Proc. Natl Acad. Sci. USA*, **104**, 997–1002.
Caufrier, F., Martinou, A., Dupont, C. & Bouriotis, V. (2003). *Carbohydr. Res.* **338**, 687–692.
Davies, G. J., Gloster, T. M. & Henrissat, B. (2005). *Curr. Opin. Struct. Biol.* **15**, 637–645.
Deng, D. M., Urch, J. E., ten Cate, J. M., Rao, V. A., van Aalten, D. M. F. & Crielaard, W. (2009). *J. Bacteriol.* **191**, 394–402.
Emsley, P. & Cowtan, K. (2004). *Acta Cryst.* D**60**, 2126–2132.
Fadouloglou, V. E., Kapanidou, M., Agiomirgianaki, A., Arnaouteli, S., Bouriotis, V., Glykos, N. M. & Kokkinidis, M. (2013). *Acta Cryst.* D**69**, 276–283.
Gill, S. C. & von Hippel, P. H. (1989). *Anal. Biochem.* **182**, 319–326.
Hernick, M. & Fierke, C. A. (2005). *Arch. Biochem. Biophys.* **433**, 71–84.
Kafetzopoulos, D., Thireos, G., Vournakis, J. N. & Bouriotis, V. (1993). *Proc. Natl Acad. Sci. USA*, **90**, 8005–8008.
Maiti, R., Van Domselaas, G. H., Zhang, H. & Wishart, D. S. (2004). *Nucleic Acids Res.* **32**, W590–W594.
Oberbarnscheidt, L., Taylor, E. J., Davies, G. J. & Gloster, T. (2007). *Proteins*, **66**, 250–252.
Psylinakis, E., Boneca, I. G., Mavromatis, K., Deli, A., Hayhurst, E., Foster, S. J., Vårum, K. M. & Bouriotis, V. (2005). *J. Biol. Chem.* **280**, 30856–30863.
Taylor, E. J., Gloster, T. M., Turkenburg, J. P., Vincent, F., Brzozowski, A. M., Dupont, C., Shareck, F., Centeno, M. S. J., Prates, J. A. M., Puchart, V., Ferreira, L. M. A., Fontes, C. M. G. A., Biely, P. & Davies, G. J. (2006). *J. Biol. Chem.* **281**, 10968–10975.
Terwilliger, T. C., DiMaio, F., Read, R. J., Baker, D., Bunkóczi, G., Adams, P. D., Grosse-Kunstleve, R. W., Afonine, P. V. & Echols, N. (2012). *J. Struct. Funct. Genomics*, **13**, 81–90.
Vollmer, W. & Tomasz, A. (2000). *J. Biol. Chem.* **275**, 20496–20501.
Vollmer, W. & Tomasz, A. (2002). *Infect. Immun.* **70**, 7176–7178.